# Post buckling of structures upon the effects of inertia

A.Combescure & J.Brochard
*CEA-CEN Saclay, IRDI/DEDR/DEMT/SMTS/LAMS, Gif-sur-Yvette, France*



The computation of post buckling of structure is considered nowadays as a solved problems. At least in the case of elastic post-buckling. The object of this paper is mainly to discuss that point and to show, from the physical point of view, and also from numerical simulations that the inertial effects cannot be omitted when one wants to predict the post buckling behaviour of a structure.

## 1. INTRODUCTION

Let us consider a structure loaded slowly by a load $\lambda$. We suppose that there is only one load parameter $\lambda$. It buckles at the load level $\lambda_c$. What is the post buckling behaviour of such a structure, just after the load $\lambda$ has reached the value $\lambda_c$ ?

## 2. QUASI STATIC POST BUCKLING METHODS

All methods for computing a static post-buckling behavior assume that the load F depends on a single parameter $\lambda$, called the load factor. That hypothesis can be written as :

(1) $F = \lambda F_0$

One has to add to the equilibrium equations a certain type of constraint.

### 2.1 Different types of constraints

The equilibrium equations written on the deformed configuration are for the load factor $\lambda$.

(2) $B^T \sigma = \lambda F_0$

B being the divergence operator written on the present configuration
$\sigma$ being the Cauchy stress tensor of this configuration

The incremental methods consists in computing the actual configuration C and the Cauchy stress tensor $\sigma$ by increasing the load factor $\lambda$ step by step [2]. All these methods fail to convergence near limit points or the bifurcation points.

To overcome this problem the general method is to add to eq. (2) the constraints :

(3) $f(U, \lambda, \Delta a, F_0) = 0$

U being the displacement field
$\lambda$ the load factor
$\Delta a$ a control parameter
$F_0$ the load vector

Constraints associated with the well known Rik's method [3] are written as :

(4) $\dot{f} = \dot{\lambda}(\lambda - \lambda_1) + \dot{U} \cdot \Delta u - \Delta a = 0$

$\dot{\lambda}$ is the gradient of load factor, and $\dot{U}$ is the gradient of displacement vector.

The constraint associated with the method proposed by BATOZ and DHATT [5] can be written :

(5) $f = \Delta\lambda\, U_q^0 + \Delta U_q^{NL} - \Delta a = 0$

This is the well known imposed displacement method. It means that the component q of the total incremental displacement is controlled, $U^0$ being the elastic linear displacement, $U^{NL}$ being the non linear part of the displacement.

STEIN [6] has imposed a constraint on the increment of external work.

(6) $f = (\Delta\lambda\, U_0 + \Delta U^{NL})\, F_0 - \Delta a = 0$

CRISTFIELD [4] has proposed the same type of method which has been used in CASTEM codes [7].

(7) $f = (\Delta\lambda\, U_0 + \Delta U^{NL}) \cdot U_1 - \Delta a = 0$

or

(8) $$\begin{cases} f = (\Delta\lambda\, U_0 + \Delta U^{NL})^T \cdot (\Delta\lambda\, U_0 + \Delta U^{NL}) - \Delta a = 0 \\ \text{with } \dfrac{(U_1,\ (\Delta\lambda\, U_0 + \Delta U^{NL}))}{\| U_1 \|\, \| \Delta\lambda\, U_0 + \Delta U^{NL} \|} > -1 \end{cases}$$

Eq (7) means that the projection of the increment of the total displacement vector $\Delta U$ on some vector (for instance the previous total displacement increment) is controlled in this form (eq. (7)) the method is a linearisation of the Rik's method.

In the form of eq. (30) the length of the displacement increment is controlled. The second condition avoids to return to the previous point of the load displacement curve.

## 3. DYNAMIC POST BUCKLING

This consist in computing the post buckling into account the inertial effects.

## 4. EXAMPLES AND DISCUSSION

We shall now compare on examples the static and dynamic post buckling prediction and show that they are rather different.

### 4.1 Example of the cylinder under external pressure.

We consider a thin rather short cylinder whose perfect geometry is given on figure 1.

The Young's modulus is E = 195 000 MPa. The Poisson's ratio is $\nu = 0.3$. The stress strain curve is given on Table 1. It is loaded by a uniform external pressure. It is clamped at its base.

The elastic bifurcation pressure is 0.04 MPa. The associated Fourier mode is 14. We choose two initial non axisymmetric imperfections which are on Fourier mode 14 but whose amplitude $\delta_0$ are either one tenth of the thickness or one time the thickness. It is meshed with eleven COMU element with response mode 0, 14, 28, 42 and 56. The imperfect structure is shown on figure 2.
The second imperfect structure (with the large imperfection) has a stable post-buckling behaviour and static and dynamic analysis give the same displacement pressure curve as can be observed from figure 3 which shows the displacement of two points A and B at an altitude of 0.5 m and at an angle of 0 and $\Pi/14$ (see figure 4).
We observe that the imperfect structure has a relatively large increase in the displacement at a pression of 0.02 MPa because of appearance of plastic hinges and finally collapses at a pressure of 0.06 MPa.
The imperfect structure with a small imperfection is analysed with Riks method. It has an unstable behaviour at an external pressure of about 0.034 MPa and a final collapse at a pressure of 0.06 MPa. The first instability is still in the elastic domain and plasticity occurs in the post-buckling path. Figure 5 gives the displacement of points A and B (experimental buckling pressure : 0.032 MPa).
The same analysis is performed taking into account the inertial effects and making the hypothesis that the external pressure is maintained constant during the post-buckling we obtain for the displacement of point A and B the curve on figure 6. By comparing these two curves we can deduce that the final shape associated with the dynamic analysis with maintained loads is much more deformed that the shape obtained with the static analysis. The buckling pressure is the same (0.034 MPa) but small vibrations just before buckling can be observed in the computation as it has been observed in experimental recording with a high speed camera.
In fact each of these two analyses correspond to the following extreme external loading situation : the first (static analysis) corresponds to a displacement controlled post-buckling whereas the second (dynamic) correspond to a load controlled post-buckling. The two loading systems are shematised on figure 7. An experimental system is somewhere in between and the observed experimental shapes are also somewhere in between.

4.2 Examples of the cylinder under axial compression. Axisymmetric post buckling (for more details see [8])

The cylinder has a radius of 75 $10^{-3}$ m, an eight of 150 $10^{-3}$ m, and a thickness of 595 $10^{-6}$ m. It is clamped at its base and submitted to an imposed displacement at its top. The mesh consist of 100 regular axisymmetric shell elements. The conventional yield stress is 142 MPa. The density is $7.810^3$ Kg/m$^3$. The Young's modulus is 82000 MPa, the Poisson's ratio 0.3. The figure 8 shows the comparison between the static and the dynamic post-buckling load deflection curve. The maximum load is the same in the dynamic and in the static case. The dynamic and static post buckling behaviour are rather different. The difference is also well represented on figure 9 where are drawn the deformed post buckled shape. The main point is that the static post buckled shape has two buckles when the dynamic one has only one buckle. The comparison with the experimental evidence shows that the dynamic simulation gives a better agreement. Figure 10 gives the post buckling shape.

4.3 Hemi-sphere under external pressure [9]

An hemi-sphere under external pressure has been computed with different types of constraints and also compared with dynamic analysis.
The sphere has a radius of 0.5 m and a mean thickness of 0.8 $10^{-3}$ m. The material has the following properties :
Youngs' modulus is 227 000 MPa, the Poisson's ratio is 0.3, the density is 7800 kg/$m^3$. The proportional yield stresses is Y = 284 MPa. Figure 11 shows the comparison between two methods of post buckling and dynamic post buckling. There is a discripency between these three results. On this curve is drown the vertical deflection of the sphere in function of the external pressure.

## 5. CONCLUSION

It has been shown that the inertial effects have a great influence on the post buckled shape. The prediction of the final shape has to take into account the inertial effects.
They also have to take into account a good model of the system of application of the loads (imposed loads or imposed displacement type of loading).
The classical post buckling strategies are to be used with care because of the inertial effects, that are always present if there is an unstable post buckling.

## REFERENCES


[1] Combescure A. Post buckling of structure, a static or a dynamic problem ? - Comput. Methods in Applied Sc. & Eng. VII - p. 593-609 (1986)
[2] Combescure A., Hoffmann A. Non linear analysis of shells : use of the equilibrium equations of the deformed body. Paper M/5-6, 5th SMiRT 1979
[3] Riks E. Incremental approach to the solution of snaping and buckling problems. Report NLR-MP-77003 U.
[4] Kriesfield M.A. Variable steplenghs for non linear structural analysis. TRRL Laboratories Reports 1049.
[5] Batoz J.L. Analyse non lineaire des coques minces elastiques. These de Docteur Ingenieur es-Sciences Universite de Laval, Quebec (Mars 1977)
[6] Stein E., Berg. A., Wagner W. Different levels of non linear shell theory in finite elements. Proc. Buckling of shells, p. 13.1 (Stuttgart, May 6-7, 1982)
[7] Combescure A. Une methode de calcul en post flambage. Rapport DEMT/SMTS/LAMS/81-058
[8] Combescure A., Bastien R. Influence des effets d'inertie sur le post flambage d'un cylindre en compression axiale. Cylindre INSA 22 01 85 Rapport DEMT 86/186
[9] Brochard J., Combescure A. Calculs en post flambage d'une cuve cylindrique en pression externe. Rapport DEMT 85/204.

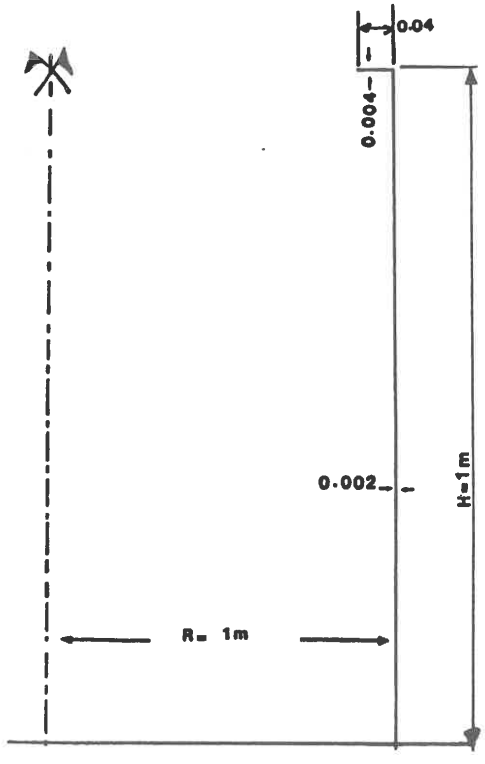


Figure 1 : Geometry (all figures in m)

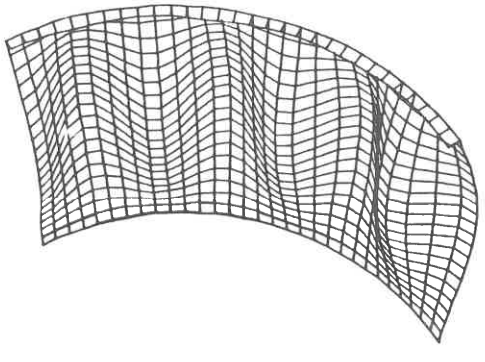

Figure 2 : Imperfect initial shapes

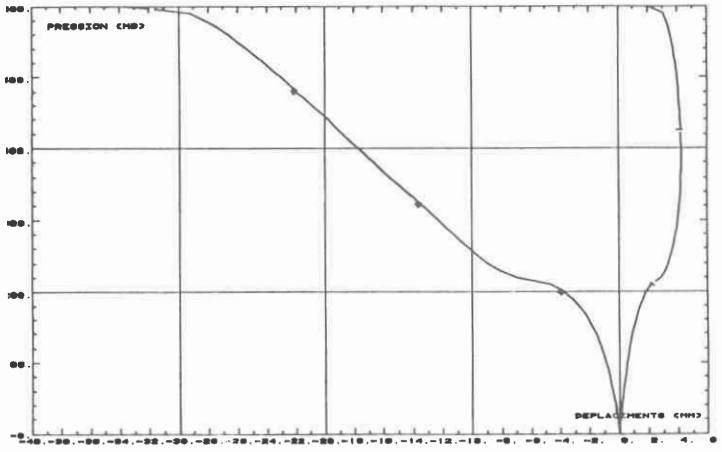


Figure 3 : Static and dynamic post buckling
Large initial imperfection $\delta_0/e = 1.$
Pressure function of radial displacement

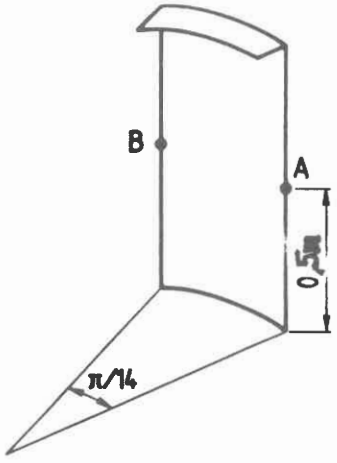


Figure 4 : Location of points A and B

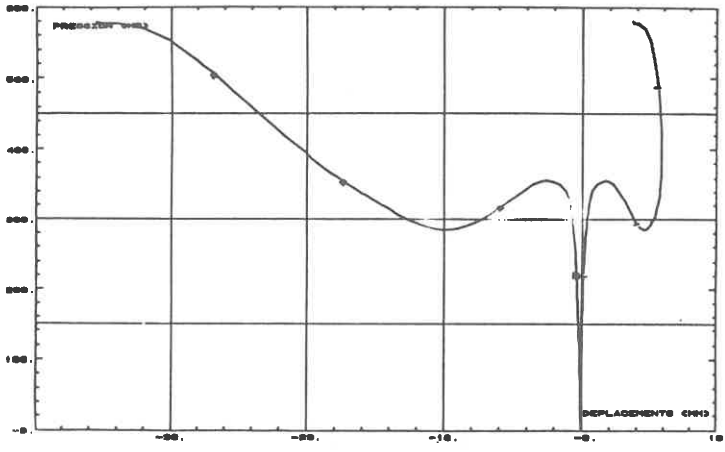

Figure 5 : Small imperfection $\delta_0/e$ = 0.1. Static post buckling

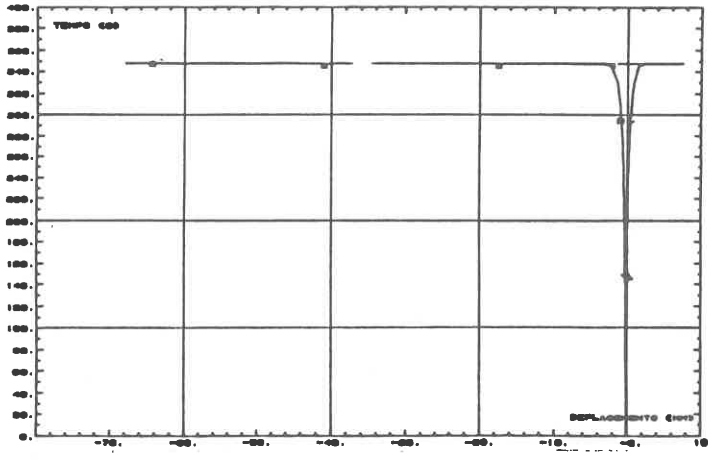

Figure 6 : Small imperfection $\delta_0/e$ = 0.1. Dynamic post buckling

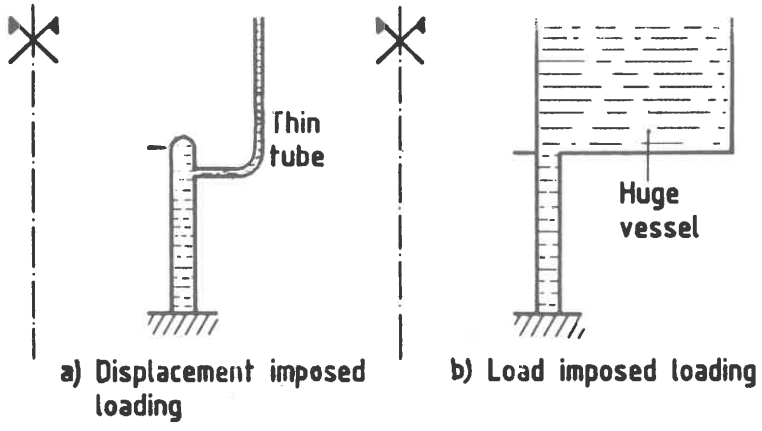


Figure 7

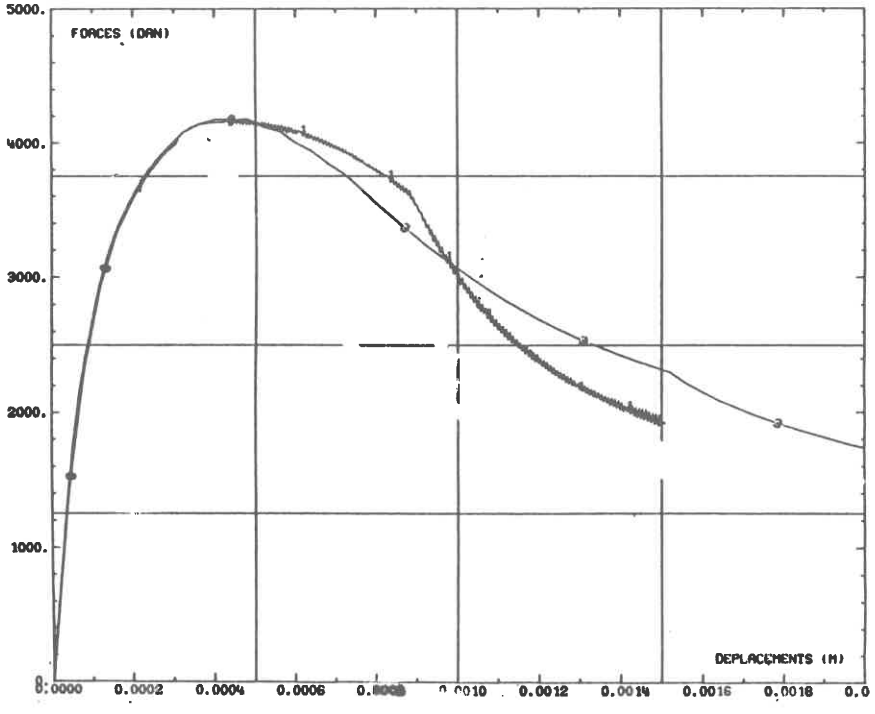


Figure 8 : Comparison of global load deflection curve

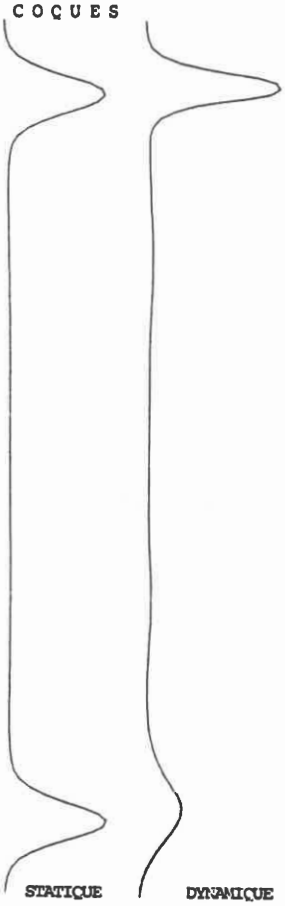


← Figure 9 : Post buckling structures

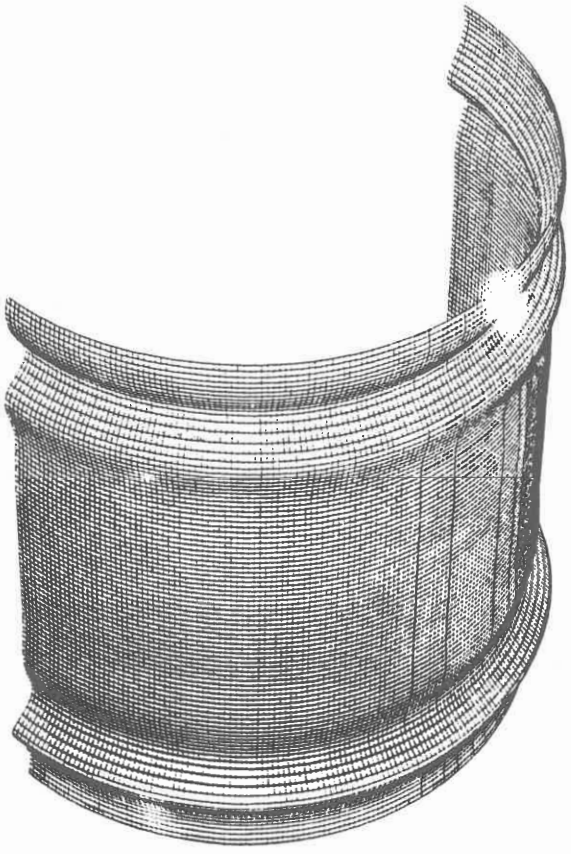

Figure 10 : Plastic buckling mode →

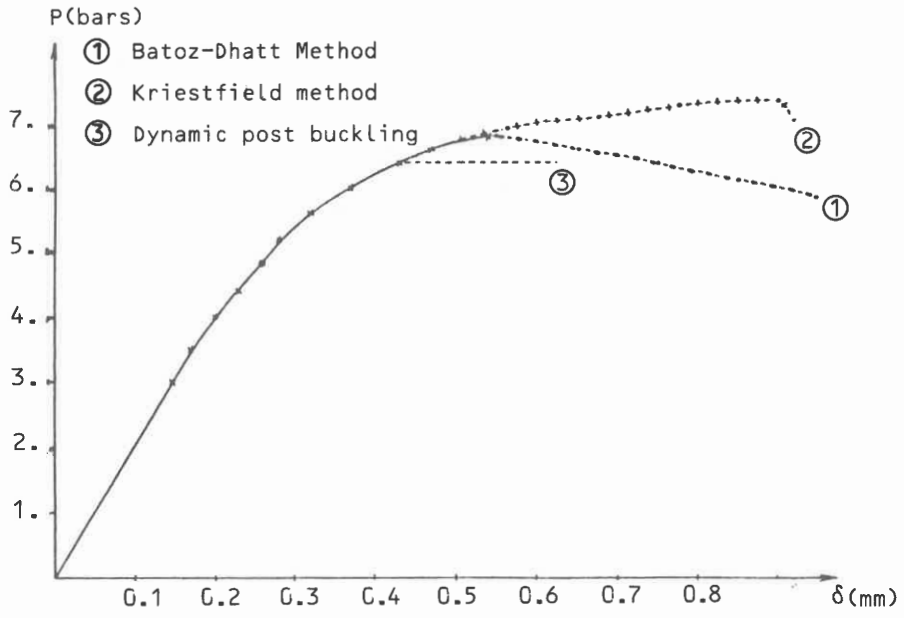


Figure 11 : Load deflection curve at the top of the hemisphere